

shi qilong (Orcid ID: 0000-0002-0089-2964)

Fang Zhongxiang (Orcid ID: 0000-0002-9902-3426)

Effects of ultrasound pretreatment on the drying kinetics, water status and distribution in scallop adductors during heat pump drying

Zhizhuang Zhu,^{a, †} Ya Zhao,^{a, †} Yuexiang Zhang,^a Xiaotian Wu,^a Jing Liu,^a

Qilong Shi^{a*} and Zhongxiang Fang^b

ABSTRACT

BACKGROUND: Material's physical and chemical properties during drying are influenced by water status and distribution. However, merely overall water removal was reported in many investigations, which hindered the clarification of drying mechanism. Therefore, effects of ultrasonic (US) pretreatment (0 W, CK; 90 W, US-90; 180 W, US-180) on the drying kinetics and quality of heat pump dried (HPD) scallop adductors was performed based on low-field nuclear magnetic resonance (LF-NMR).

RESULTS: Compared with CK, effective moisture diffusion coefficient was increased

*Correspondence to: Qilong Shi, School of Agricultural Engineering and Food Sciences, Shandong University of Technology, Zibo 255000, P.R. China.

E-mail address: shiqilong2006@hotmail.com

† Zhizhuang Zhu and Ya Zhao contributed equality to this work and are co-first authors.

^a Department of Food Science and Engineering, School of Agricultural Engineering and Food Sciences, Shandong University of Technology, Zibo, P.R. China

^b School of Agriculture and Food, The University of Melbourne, Parkville, Vic 3010, Australia

This is the author manuscript accepted for publication and has undergone full peer review but has not been through the copyediting, typesetting, pagination and proofreading process, which may lead to differences between this version and the Version of Record. Please cite this article as doi: [10.1002/jsfa.11290](https://doi.org/10.1002/jsfa.11290)

This article is protected by copyright. All rights reserved.

by 12.43% and 23.35% for US-90 and US-180, respectively. The Weibull model satisfactorily described the drying characteristics with a high R^2 (>0.998), low $RMSE$ (<0.0120) and χ^2 (<0.00008). LF-NMR revealed that the immobilized water was predominant in scallop adductors. As drying proceeded, the relaxation time of free and immobilized water was decreased sharply, whereas the relaxation time of bound water was hardly changed. The time required to reduce approximately two fifths of original peak area of immobilized water was 720, 630, and 540 min for CK, US-90 and US-180, respectively. The amplitude of immobilized water was decreased and bound water increased significantly, but free water was kept constant (ranging 1–2%). US pretreatment reduced total color difference and hardness, but enhanced toughness of dried scallop adductors. However, US had no significant influence on the product rehydrate rate and shrinkage rate.

CONCLUSION: LF-NMR was successfully employed to evaluate the drying degree of scallop adductors. US facilitated the conversion of immobilized water to free water, and consequently promoted the water removal during HPD.

Keywords: drying; LF-NMR; scallop adductors; ultrasound; water state and distribution; Weibull model

INTRODUCTION

Scallops (*Argopecten irradians*) are not only an important fishery resource in the world marine ecosystem, but also an aquatic product with great commercial value. In China, scallops are a preferential target in the aquaculture because of their rapid growth rate, high reproduction rate.¹ Scallop adductors are the main edible and processed portion of scallops with high nutritive value and health care function.² However, the shelf life of scallop adductors is limited owing to its high moisture content (MC, usually higher than 800.0 g water kg⁻¹ fresh sample) and water activity (a_w), and susceptible to quality deterioration.³

Drying is a commonly employed method aiming at removing the MC and lowering the a_w of foodstuffs, and is applied predominately for perishable foods such as fruits, vegetables, and aquatic products.⁴ Traditional drying methods such as hot air drying have drawbacks in practice including low drying efficiency, inferior quality attributes, and severe volume shrinkage caused by high drying temperature.^{3, 5} Therefore, lowering the temperature of drying medium will have enormous potential in enhancing the quality of dried products.

Heat pump drying (HPD), the integration of a heat pump system and a traditional convection (or infrared radiation) drying chamber, is suitable for drying heat-sensitive foods especially aquatic products.⁶ Higher energy efficiency, mild drying conditions (viz. drying temperature 10 – 55 °C and relative humidity [RH] 10 – 50%), improved product quality, and environmentally friendly are the advantages of HPD over other

traditional convection drying techniques.⁷ However, there are some drawbacks of HPD including lower drying rate and higher energy consumption at the later drying stage, which restrict its applications.⁷ To overcome the shortcomings of HPD, researches have been focused on the advanced technologies that can improve drying efficiency, lower energy consumption, and enhance quality attributes.⁵

Pretreatment is an important unit operation commonly employed before drying to increase the drying efficiency. Chemical pretreatments include liquid treatment (e.g. hyperosmotic solution, sulfite solution), gas treatment (e.g. ozone, carbon dioxide), and other methods (e.g. ethanol, edible coatings).⁸ However, these methods might have food safety issues caused by chemical residuals and water-soluble nutrients loss during the operation.⁸ Physical pretreatments include thermal blanching and other methods such as peel abrasion, skin puncturing.⁸ Non-thermal physical pretreatments such as freeze-thaw, pulsed electric field, high hydrostatic pressure, and ultrasound (US) can improve drying efficiency, inactivate enzymes while avoiding the detrimental influences of heat on the nutritive components and sensory properties of foods compared to the thermal ones.⁸⁻¹⁰

US is an environmentally friendly and non-thermal technique that can save energy, reduce processing time, enhance product quality, and extend shelf life.¹¹ US can be classified into three categories based on frequency, viz. power US (20 – 100 kHz), high-frequency ultrasound (100 kHz – 1 MHz), and diagnostic US (1 – 500 MHz). High-frequency and diagnostic US are usually utilized for analyzing material's

physicochemical properties, and monitoring food changes during processing; whereas, power US is employed to break down cellular structure for triggering and inhibiting physical and/or chemical changes in foods, resulting intensified heat and mass transfer during processing.⁵ US is generally employed in food industry for disinfection, sterilization, enzyme inactivation, desensitization, dehydration, curing, tenderization and cooking, and etc.¹¹ US-assisted drying is promising especially for heat-sensitive materials because of markedly accelerated drying process without causing a noticeable increase in the material's temperature.¹² Numerous investigations have been reported on US-assisted drying of fruits and vegetables, such as US-assisted convective drying of strawberry,^{13, 14} raspberries,¹⁵ green pepper,¹⁶ garlic,¹⁷ kiwifruit;¹⁸ US-assisted conductive drying of apple;¹⁹ US-assisted infrared drying of carrot,²⁰ garlic,²¹ potato;²² US-assisted microwave drying of daylilies,²³ and microwave-assisted freeze-drying of Chinese yam.²⁴ However, only a few works have been performed on US-assisted drying of protein-rich foodstuffs such as beef and chicken,²⁵ codfish,²⁶ salmon and trout.²⁷ Furthermore, the above researches mainly focused on the parametric influences of US treatment (e.g. US power, sonication time) and drying-related conditions (e.g. drying temperature, velocity) on the drying kinetics and quality attributes.^{12, 28} It is well known that material's physical and/or chemical properties during drying are significantly affected by the water status and distribution, and its interactions with materials' microstructure.²⁹ However, in most of the investigations, merely overall water removal process was reported, which hindered the clarification of mechanism of

US-assisted drying.

Low-field nuclear magnetic resonance (LF-NMR), measuring the resonant ratio frequency absorption by non-zero nuclear spins under the circumstance of an external static magnetic field, has been increasingly used as a sensitive, fast, and non-destructive analytical method for the characterization of water mobility and distribution within food matrix.^{30, 31} Specifically, LF-NMR has been widely applied to investigate the MC, a_w , water state and distribution during drying of fruits and vegetables, such as broccoli,²⁹ garlic,¹⁷ kiwifruit,¹⁸ Chinese yam.³² However, only a few studies have been performed for monitoring the water state and distribution during drying of aquatic products, such as hot air drying of abalone,³³ oyster,³⁰ shrimp;³⁴ explosion puffing drying of scallop adductors.³ To the best of our knowledge, there is little information about US-assisted HPD kinetics of scallop adductors based on LF-NMR. Therefore, the purposes of this work were to: (1) explore the effectiveness of US pretreatment on the drying kinetics and quality attributes of scallop adductors during HPD; (2) reveal the effect of US pretreatment on the water state and distribution of scallop adductors during HPD; and (3) correlate the MC of scallop adductors with LF-NMR relaxation signal.

MATERIAL AND METHODS

Sample preparation

Fresh scallops were purchased from a local market (Zibo, China). After washing, shelling, skirt-removing, the adductor muscles were collected. The average length, diameter and mass (n=20) of scallop adductors were 2.11 ± 0.08 cm, 1.80 ± 0.14 cm

and 3.93 ± 0.47 g, respectively. The average initial MC in wet basis (w.b.) of fresh scallop adductors was 812.6 ± 2.1 g water kg^{-1} fresh sample as measured gravimetrically by drying the samples in an oven (DHG-9140A, Yiheng Scientific Instrument Co. Ltd., Shanghai, China) at $100\text{ }^{\circ}\text{C}$ until constant weight. The protein, fat, and ash content of scallop adductors were 127.5 ± 12.3 , 27.3 ± 3.2 , and 12.9 ± 2.6 g kg^{-1} fresh sample, respectively.

Ultrasound (US) pretreatment

All the US pretreatments were carried out in an ultrasonic apparatus (SK3310LHC, Kudos Ultrasonic Instrument Co., Ltd, Shanghai, China) with the frequency of 35 kHz and power capacity of 180 W. The following treatments were carried out: (1) scallop adductors treated with US power 0 W, viz. without US treatment (coded as “CK”); (2) scallop adductors treated with US power 90 W (coded as “US-90”); (3) scallop adductors treated with US power 180 W (coded as “US-180”). For each treatment, scallop adductors (~ 100 g) were placed in a 500 mL beaker containing distilled water and put in the ultrasonic bath. The weight ratio of scallop adductors to distilled water was maintained at 1:4. The processing temperature and time of US treatment was $28 \pm 2\text{ }^{\circ}\text{C}$ and 30 min, respectively. During US process, an ice-cold water was used to maintain the temperature of the water in the beaker. After each pretreatment, the scallop adductors were taken out and gently wiped with filter paper to remove the surface water on the adductors. Finally, the scallop adductors with and without US pretreatments were further dried in a heat pump drier/dehumidifier.

Heat pump drying (HPD)

Scallop adductors with and without US pretreatments were dried in a laboratory scale heat pump drier (1HP-5, Qingdao Oumeiya Technology Co. Ltd., Qingdao, China). The schematic diagram and principle of heat pump dryer were illustrated in our previous research. ⁶ Briefly, the samples were dried at our preliminarily tested parameters of temperature 35 °C, air velocity 1.5 m s⁻¹, RH 40 – 60%, and evaporator bypass air ratio 0.6 – 0.8. After the conditions of the dryer were stabilized (approximately 30 min), the scallop adductors were weighted and distributed uniformly on the stainless-steel grid trays. Drying process of scallop adductors was accomplished once the sample's MC in dry basis (d.b.) reached approximately 0.9 kg water kg⁻¹ scallop. The dried scallop adductors were immediately packed using aluminum laminated packs, placed in a desiccator containing excess silica gel, and maintained at 5 ± 1 °C for further quality analyses. All the drying process were carried out in triplicate.

Drying kinetics and mathematical modeling

Drying kinetics

The moisture ratio (*MR*) and drying rate (*DR*) of scallop adductors during HPD were calculated using Eqs. (1) and (2), respectively: ²

$$MR = \frac{M_t - M_e}{M_0 - M_e} \quad (1)$$

$$DR = -\frac{dM_d}{dt} = -\frac{M_{d,i+1} - M_{d,i}}{t_{i+1} - t_i} \quad (2)$$

where M_t , M_0 , and M_e are, respectively, the MC (kg water kg⁻¹ scallop, d.b.) at drying

time of t , the initial MC, and the equilibrium MC; $M_{d,i}$ and $M_{d,i+1}$ are, respectively, the MC (kg water kg⁻¹ scallop, d.b.) of scallop adductors at time t_i and t_{i+1} ; t is drying time (h). MR is usually simplified as $MR=M_t/M_0$ due to negligible of M_e value comparing M_t and M_0 .⁶

Mathematical modeling fitting

Weibull distribution model was used to fit the drying kinetics data and can be expressed in the following equation:^{35, 36}

$$MR = \exp \left[- \left(\frac{t}{\alpha} \right)^\beta \right] \quad (3)$$

where α and β are, respectively, the scale (min) and shape (dimensionless) parameters of the Weibull model; t is the drying time (min).

The coefficient of determination (R^2), reduced chi-square (χ^2), and root-mean-square error ($RMSE$) between the experimental and predicted data were used to evaluate the accuracy of the model fitting.^{6, 35}

Calculation of effective moisture diffusion coefficient (D_{eff})

The D_{eff} is an important moisture transport performance in drying of agro-products and is a function of drying temperature and MC in the matrix.⁶ For most convective drying, it is in the falling rate period that drying mainly occurs in which the internal moisture and/or vapor diffusion is the dominate moisture transfer controlling mechanism.⁶ The D_{eff} of scallop adductors during HPD was calculated according to the simplified Fick's diffusion model:²

$$MR = \frac{6}{\pi^2} \sum_{n=0}^{\infty} \frac{1}{n^2} \exp\left(-\frac{n^2 \pi^2 D_{eff} t}{r^2}\right) \quad (4)$$

where n is the positive integer, r is the radius of adductors (m), and t is drying time (s).

The simplified logarithmic form of Eq. (4) can be used to express the linear relation between MR and t , and the equation can be observed by Eq. (5):²

$$\ln MR = \ln\left(\frac{6}{\pi^2}\right) - \left(\frac{\pi^2 D_{eff}}{r^2}\right) t \quad (5)$$

By plotting $\ln MR$ versus t , D_{eff} can be calculated from the slope.

LF-NMR transverse relaxation analysis

The spin-spin relaxation time measurements were performed on a LF-NMR analyzer (PQ001, Niumag Co. Ltd., Shanghai, China) with a resonance frequency for protons of 20 MHz at 32 °C. The scallop adductors were placed into a 25-mm diameter cylindrical glass tube and inserted in the NMR sample holder. The transverse relaxation time T_2 was measured using Carr-Purcell-Meiboom-Gill (CPMG) pulse sequence and typical pulse parameters were as follows: 4000 ms waiting time, 2000 echoes, 5.52 and 11.04 μ s for 90° and 180° pulse width, respectively. The NMR relaxation curve was fitted to a multi-exponential curve using the in-built Multi-Exp Inv analysis software.³

Quality analyses

Shrinkage rate (S_R)

The S_R of scallop adductors was determined using the method of Shi *et al.*²

$$S_R(\%) = \frac{V_1 - V_0}{V_0} \times 100 \quad (6)$$

where V_1 and V_0 are, respectively, the volume of scallop adductors before and after HPD.

Rehydration ratio (R_R)

The R_R of scallop adductors was determined using weighing method according to Shi *et al.*² The R_R was calculated using Eq. (7):

$$R_R = \frac{W_r}{W_d} \quad (7)$$

where W_d and W_r are, respectively, the mass of samples before and after rehydration.

Color parameters

A colorimeter (WSC-S, Shanghai Physical Optics Instrument Co. Ltd., Shanghai, China) was used to measure the color parameters of scallop adductors. The total color difference (ΔE) of scallop adductors was calculated using Eq. (8):⁶

$$\Delta E = \sqrt{(L - L^*)^2 + (a - a^*)^2 + (b - b^*)^2} \quad (8)$$

where L^* , a^* , and b^* are the color parameter of fresh scallop adductors; L , a , and b are the color parameters of scallop adductors after HPD.

Texture profile measurements (hardness and toughness)

The texture properties (viz. hardness and toughness) of scallop adductors were measured using a texture analyzer (TA.XT plus, Stable Micro Systems Ltd., Godalming, UK). The shear and uniaxial compression test were carried out according to the methods of Shi *et al.*² and Cheng *et al.*³⁴ Hardness and toughness determinations were performed with the in-built expert software.

Statistical analysis

The experimental runs were performed in triplicates and the data were expressed as mean \pm standard deviation. The linear and non-linear regression analysis were

accomplished using Matlab 7.1 software (Mathworks Inc., Natick, MA, USA). Analysis of variance (ANOVA) was fulfilled using SPSS software (Version 21.0, SPSS Inc., Chicago, USA). Duncan's multiple range test was used to evaluate the differences between means at 95% confidence interval. Pearson correlation analysis and principal component analysis (PCA) were performed using Origin software (Version 8.5, MathWorks Corp., Natick, MA, USA).

RESULTS AND DISCUSSION

Drying kinetics

The effect of US pretreatment on the drying curves of scallop adductors is shown in Fig. 1(a). *MR* was decreased exponentially with drying time for fresh and US treated scallop adductors. As can be deduced from Fig.1(a), US power has a positive effect on the drying kinetics of scallop adductors. For example, to achieve the MC of 1.30 water kg⁻¹ scallop (d.b.), the drying time for scallop adductors without US pretreatment (i.e. CK) was 454 min. However, when US pretreatment was employed, the drying time was reduced to 373 and 346 min for US-90 and US-180, respectively, with the time decreasing rate of 17.84% and 23.79%, respectively. Similar decreasing tendency in drying time with application of US was reported in convective drying of desalted codfish,²⁶ infrared drying of carrot slices,²⁰ and pulsed fluidized bed microwave freeze-drying of Chinese yam.²⁴ During drying, water is migrated within the material to its surface (viz. internal moisture flux), and then released to the surroundings via the boundary layer of the heating medium (viz. external moisture flux).¹² The increment

in the internal and external moisture flux with the application of US was attributed to the desirable generation of microscopic channels induced by sponge effect (i.e. successive compression and expansion of the sample) and cavitation phenomenon (i.e. the breaking of vapor bubbles near the water surface) which resulted in a decrease in surface tension that facilitated the removal of water.¹²

Based on the kinetic theory, the drying process consists of three stages, the first stage (i.e. the induction period) where the water flow mechanisms are involved; the second stage (i.e. the constant drying rate period) corresponds to the period in which the maximum drying rate are achieved; and the third stage (i.e. the falling drying rate period) where the water flux from the inside to the material's surface is smaller than the rate of surface water evaporation.³⁷ The influence of US pretreatment on the *DR* curves of scallop adductors is shown in Fig. 1(b). In general, the overall drying process was determined in the falling rate period, which demonstrated that the drying process of scallop adductors was controlled by internal moisture diffusion. It was obvious that the *DR* of scallop adductors was enhanced by US pretreatment. The higher the US power, the higher drying efficiency was achieved. Furthermore, *DR* exhibited a declining tendency with the decrease of MC (d.b.). For instance, at the initial stage of drying (e.g., MC of approximately 4.0 kg water kg⁻¹ scallop), the average *DR* of scallop adductors was increased by 16.53% and 95.04% for US-90 and US-180, respectively, compared with HPD alone (CK). When the MC of scallop adductors was reduced to 2.0 kg water kg⁻¹ scallop, the corresponding average *DR* was increased by 23.33% and 36.67% for

US-90 and US-180, respectively, compared with CK. However, when the MC of scallop adductors was lower than 1.0 kg water kg⁻¹ scallop, all the *DR* curves inclined to overlap. This finding implied that the enhancement effect of US was closely related to the MC of scallop adductors. Comparable observations also have been demonstrated by Bantle and Eikevik³⁸ for ultrasound assisted convective drying of clipfish, and Xi *et al.*²² for ultrasonic wave assisted far-infrared drying of potato.

Mathematical modeling fitting

Nonlinear regression was employed to fit the experimental *MR* data to the Weibull model, and the model parameters and statistical test are listed in Table 1. As can be seen, the R^2 value of all treatments was identical ($R^2=0.999$). However, the χ^2 and *RMSE* values were observed to be vary from 7.143×10^{-5} to 8.140×10^{-5} , and 0.0107 to 0.0120, respectively. The higher the R^2 value, and the lower the χ^2 and *RMSE* values signify an excellent model fit to the experimental data. Therefore, the Weibull model was demonstrated to be suitable in predicting the *MR* of scallop adductors (with and without US pretreatment) at drying air temperature of 35 °C and air velocity of 1.5 m s⁻¹.

Table 1 also shows that the scale parameter (α) and the shape parameter (β) of the Weibull model ranged from 246.92 ± 14.77 to 322.57 ± 19.39 min, and from 0.60 ± 0.07 to 0.69 ± 0.03 , respectively. The scale parameter α defines the *DR* and represents the time required to accomplish 63% of the drying process.³⁶ The lower the α value, the higher the water removal rate during drying. It can be seen from Table 1 that the α values of US pretreated scallop adductors were significantly ($p<0.05$) lower than CK.

For the US pretreated samples, the α value was significantly ($p<0.05$) decreased with the increase of US power.

The shape parameter (β) is closely related to the mass transfer velocity at the beginning of drying, viz. the higher the β value, the slower the DR at the beginning³⁵. There was no significant difference ($p>0.05$) in β value between scallop adductors with and without US pretreatment (Table 1). During drying, various mechanisms (such as diffusion, convection, and relaxation) can be deduced from the drying curves based on the β value.³⁹ According to the β value, drying behavior can be classified into three types: when $\beta<1$, the drying process belongs to falling rate period; when $\beta=1$, the DR is constant over time, and the drying characteristic is considered to be first order kinetics; whereas, when $\beta>1$, the DR increases over time during a certain time span.⁴⁰ In the present study, the β value below 1.00 was observed in all cases, which indicated that the drying behavior of scallop adductors (with and without US pretreatment) was typical of falling rate process. This finding was in well accord with the DR curves exhibited in Fig.1(b).

The effective moisture diffusivity coefficient (D_{eff}) was determined by Fick's diffusion model, and the results are shown in Table 1. The D_{eff} value of scallop adductors ranged from 2.933×10^{-10} to 3.692×10^{-10} $m^2 s^{-1}$. The enhanced drying efficiency of scallop adductors during HPD was observed for the US pretreatment. Compared with CK, the D_{eff} value was increased by 12.43% and 23.35% for US-90 and US-180, respectively. These results were in well agreement with above drying kinetics

of scallop adductors. Similar increasing tendency in D_{eff} with the application of US was observed in convective drying of desalted cod.²⁶

Water state and distribution in scallop adductors based on LF-NMR

NMR transverse relaxation of fresh scallop adductors

The proton spin-spin relaxation time (T_2) can be employed to investigate the mobility and freedom degree of water molecules, and indirectly exhibit the dynamic properties of water molecules (e.g. water diffusion and state distribution) during drying.³ The relaxation component (T_2) and corresponding peak area fractions (A_2) reflect the water state and distribution in the scallop adductors. A representative NMR transverse relaxation time (T_2) spectra of fresh scallop adductors is shown in Fig. 2. Three distinct peaks can be observed with the relaxation time of approximately 5.6, 61.5, and 871.9 ms, respectively. In fresh scallop adductors three water state can be observed, viz. bound water (T_{21} , 0 – 10 ms) which is tightly attached to macromolecules; immobilized water (T_{22} , 10 – 100 ms) which is entrapped within extra-myofibrillar lattice, and free water (T_{23} , 100 – 1000 ms) which exists in the myofibril lattice.³ The peak area of the relaxation components is proportional to the total MC in the matrix.³⁰ The corresponding peak area fraction of three peaks is, respectively, coded as A_{21} , A_{22} and A_{23} , which represent the percentage of bound water, immobilized water, and free water.

³ In terms of the water state distribution, the values of A_{21} , A_{22} and A_{23} for fresh adductors were 0.78%, 98.18%, and 1.04%, respectively. Therefore, most of the water in fresh scallop adductors was non-flowable water or immobilized water that entrapped

within extra-myofibrillar lattice. In harmony with these data, the dominant role of immobilized water in protein-based food was also observed in shrimp,³⁴ chicken breast,⁴¹ beef jerky,³¹ and golden pompano fillets.⁴² However, for fresh pacific oyster, only one relaxation population (approximately 350 ms) was distinguished, which was ascribed to the free water.³⁰ The reason for this discrepancy may be the differences in material's chemical composition and physical structure which affects the binding force between water and non-aqueous components.

NMR transverse relaxation of scallop adductors during HPD

The effect of US pretreatment on the water state and distribution is shown in Fig. 3. As can be seen, T_{21} hardly changed ($p>0.05$) for all the treatments during drying period of 0 – 5 h, and was in the range of 5.60 – 5.60 ms, 5.87 – 5.11 ms, and 5.60 – 5.11 ms for CK, US-90, and US-180, respectively. This finding demonstrated that the bound water in scallop adductors was strongly associated with macromolecular (e.g. protein), and the mobility of bound water in muscle tissue was not influenced by the prolonged drying time especially at the initial drying stage. Afterwards, T_{21} of scallop adductors was significantly ($p<0.05$) decreased to 3.51 ms at the end of drying, viz. drying time of 13, 11, and 11 h for the treatment of CK, US-90, and US-180, respectively. Furthermore, it was observed that the curves of T_{22} and T_{23} shifted leftwards and the peak areas gradually decreased with the increasing drying time for all the treatments, which signified more tightly binding degree between water and non-aqueous components.⁴² For example, the values of T_{22} for scallop adductors without US pretreatment were

61.51, 45.45, 39.53, 36.01, 27.24, 23.70, and 18.86 ms, respectively, when dried at 1, 3, 5, 7, 9, 11, and 13 h. In contrast, the values of T_{23} for scallop adductors without US pretreatment were 871.87, 775.91, 710.07, 560.31, 464.16, 403.70, and 377.41 ms, respectively, when dried at the same time intervals. Similarly, the phenomenon that hardly any left shift of T_{21} , and sharply decreased of T_{22} and T_{23} with the increase of drying time were reported in hot air drying of shrimp.³⁴

Water distribution of scallop adductors during HPD

The variation of water state proportion can be calculated based on the total signal intensity alternations of water in different states in T_2 inversion spectrum. The evolution of water state distribution during HPD is shown in Fig. 4. During the whole period of drying, the proportion of immobilized water (A_{22}) was sharply ($p < 0.05$) decreased for all the samples. The time required to reduce approximately two fifths of the original peak area of A_{22} was observed to be 720, 630, and 540 min, respectively, for samples of CK, US-90, and US-180. This finding implies that the higher the US power, the faster the migration rate of immobilized water and free water, and the shorter the drying time. As mentioned above, the formation of microscopic channel induced by sponge effect and cavitation phenomenon of US pretreatment facilitate the conversion of immobilized water to free water, and ultimately promoted the water removal during drying.¹² The peak area and proportion of bound water (A_{21}) were increased with increasing drying time especially at the later drying stage. For example, at drying time of 10 h, the proportion of T_{21} of scallop adductors were 24%, 22%, and 22%, respectively, for

Author Manuscript

samples of CK, US-90, and US-180. The reason might be the conversion of part of immobilized water into bound water. Furthermore, the peak area and proportion of free water (A_{23}) for all the treatments tended to be constant (ranging 1 – 2%) with increasing drying time despite the fact that T_{23} decreased sharply with drying proceeded. The reason may be that a relative dynamic equilibrium state was achieved between the removal rate of free water and the conversion rate of bound water to free one as a result of the mild drying conditions of HPD. Similar increasing trend of bound water proportion, decreasing trend of immobilized water proportion, and insignificant variation of free water proportion with increasing drying time were observed in convective drying of oyster,³⁰ chicken jerky,⁴¹ and beef jerky.³¹

Correlation analysis between NMR relaxation parameters and MC of scallop adductors

Pearson correlation coefficient was analyzed to determine the relevance between NMR relaxation parameters and total MC of scallop adductors, and the results are shown in Fig.5. The immobilized water (T_{22}) was significantly correlated with the total MC of scallop adductors during HPD. The corresponding correlation coefficients (R^2) were 0.967, 0.976, and 0.985 for treatments of CK, US-90, and US-180, respectively. This finding was coincident with the aforementioned fact that the immobilized water was the dominating water state and determined the variations in the MC of scallop adductors during HPD process. Therefore, LF-NMR can be employed to rapidly and non-destructively monitor the drying degree of scallop adductors. Similar strong correlation

between NMR relaxation parameter T_{22} and the MC was reported in convective drying of abalone,³³ chicken jerky,⁴¹ and oyster.³⁰

PCA analysis based on NMR parameters

PCA is a mathematical method for dimensionality reduction and is a powerful statistical means for combining the original variables into a new group of independent comprehensive variables. The PCA was carried out on the whole CPMG relaxation curves of scallop adductors (with and without US pretreatment) at different MC levels to distinguish the drying degree of samples. The score plots of the first two principal components, viz. PC1 and PC2 are shown in Fig.6. Scallop adductors with different MC (w.b.) ranges were marked with different symbol, viz. M4 (MC 400 – 500 g water kg⁻¹ fresh sample), M5 (MC 500 – 600 g water kg⁻¹ fresh sample), M6 (MC 600 – 700 g water kg⁻¹ fresh sample), M7 (MC 700 – 800 g water kg⁻¹ fresh sample). It was observed that the cumulative contribution of PC1 and PC2 represented 90.1% of the total variance. The samples with different MC levels can be completely divided into three portions using three dashed ellipses (Fig.6). This finding demonstrated that MC levels of scallop adductors had significant ($p < 0.05$) influence on the transverse relaxation performance of samples. In addition, the three portions that were clearly separated from each other were M7, M6 – M5, and M4, respectively, which were corresponded to the initial, middle and final stage of drying process. The scallop adductors of M7 (viz. drying time < 2 h) and M4 (viz. drying time > 8 h) showed perfect separation, whereas the samples of M6 – M5 (viz. dried at 2 – 8 h) was not be

distinguished. The PCA demonstrated that different drying stages could be distinguished by LF-NMR data. Similar close correlation between LF-NMR and drying procedure was reported in convective drying of pacific oyster,³⁰ and microwave drying of Chinese yam.³²

Quality attributes of scallop adductors

The effects of US pretreatment on the quality attributes of dried scallop adductors, viz., ΔE , R_R , S_R , hardness, and toughness are listed in Table 2. Color variation of dried aquatic products is a crucial indicator for the food quality.²⁸ Compared with CK, the ΔE of dried scallop adductors was significantly ($p < 0.05$) decreased from 18.03 ± 0.09 to 15.20 ± 0.89 when US power was increased from 0 to 90 W. Further increasing US power to 180 W led to continuously ($p < 0.05$) decreased ΔE of 13.00 ± 0.67 . The reason may be the shortened drying time of the scallop adductors during HPD with US pretreatment. Similar decreasing trend of ΔE with US pretreatment was observed for convective drying of raspberries,¹⁵ green pepper,¹⁶ and red beetroot.⁴³ The hardness of scallop adductors was significantly ($p < 0.05$) decreased from 151.52 ± 5.26 g to 128.52 ± 1.20 g when US power was increased from 0 to 180 W. However, there was no significant difference ($p > 0.05$) in hardness for treatment of CK and US-90, US-90 and US-180, respectively. Compared with the CK, the toughness of scallop adductors was significantly ($p < 0.05$) increased with US power of 90 W. However, further increasing US power to 180 W exhibited insignificant ($p > 0.05$) impact on toughness. Similar decreasing tendency in hardness with US were observed in drying of red

Author Manuscript

beetroot,⁴³ and salted cod.⁴⁴ Compared with the CK, the S_R of dried scallop adductors decreased by 0.42% and 0.20% for treatment of US-90 and US-180, respectively. By contrast, the R_R of dried scallop adductors was decreased 1.69%, and increased 0.85% for treatment of US-90 and US-180, respectively. However, no significant differences ($p>0.05$) were observed in R_R and S_R for treatments of CK, US-90, and US-180, respectively. Gamboa-Santos *et al.*¹⁴ demonstrated that there were no significant differences in R_R between convective dried strawberries with and without US treatment. Similarly, the application of US during convective drying of strawberry exhibited negligible influence on the volume shrinkage.¹³

CONCLUSIONS

The drying process of scallop adductors was driven by internal moisture diffusion. The reinforcement influence of US on the drying behavior of scallop adductors became stronger with the increase of US power. Compared with CK, the D_{eff} value was increased by 12.43% and 23.35% for treatment of US-90 and US-180, respectively. The Weibull model was suitable for describing the drying behavior of scallop adductors. The scale and shape parameters of Weibull model ranged from 257.37 to 322.57 min, and from 0.60 to 0.69, respectively. There were three water components (*viz.* bound, immobilized, and free water) and immobilized water was predominant in fresh scallop adductors. As the drying process proceeded, the relaxation time of immobilized water and free water decreased sharply. However, there was little change in the relaxation time of bound water. The immobilized water was the main component that being removed during HPD.

The higher the US power, the faster the migration rate of immobilized water and free water, and the shorter the drying time. LF-NMR was a useful tool in evaluating drying degree of scallop adductors. US pretreatment decreased the ΔE , hardness, and increased toughness of dried scallop adductors. However, US had no significant influence on the rehydrate rate and shrinkage rate of dried scallop adductors. Overall, US-180 pretreatment is recommended for HPD of scallop adductors with enhanced drying efficiency and improved quality attributes.

DECLARATION OF COMPETING INTEREST

The authors declare no conflicts of interest.

ACKNOWLEDGEMENTS

This study was supported by Shandong Provincial Natural Science Foundation (ZR2020MC215).

REFERENCES

1. Zhao X, Liu Y, Wang G, Tao W, Lou Y, Li N and Liu Y, Tracing the geographical origins of Yesso scallop (*Patinopecten yessoensis*) by using compound-specific isotope analysis: An approach for overcoming the seasonal effect. *Food Control* **102**:38-45 (2019).
2. Shi Q, Tian Y, Zhu L and Zhao Y, Effects of sodium alginate-based coating pretreatment on drying characteristics and quality of heat pump dried scallop adductors. *J Sci Food Agr* **99**:4781-4792 (2019).
3. Sui X, Zhao Y, Zhang X, Zhang Y, Zhu L, Fang Z and Shi Q, Hydrocolloid coating pretreatment makes explosion puffing drying applicable in protein-rich foods – A case study of scallop adductors. *Drying Technol* DOI: 10.1080/07373937.2020. 1768108 (in press). (2020).
4. Duan X, Yang X, Ren G, Pang Y, Liu L and Liu Y, Technical aspects in freeze-drying of foods.

Drying Technol **34**:1271-1285 (2015).

5. Dehghannya J, Kadkhodaei S, Heshmati MK and Ghanbarzadeh B, Ultrasound-assisted intensification of a hybrid intermittent microwave - hot air drying process of potato: Quality aspects and energy consumption. *Ultrasonics* **96**:104-122 (2019).
6. Shi Q, Zheng Y and Zhao Y, Mathematical modeling on thin-layer heat pump drying of yacon (*Smallanthus sonchifolius*) slices. *Energy Convers Manage* **71**:208-216 (2013).
7. Shi Q, Zheng Y and Zhao Y, Optimization of combined heat pump and microwave drying of yacon (*Smallanthus sonchifolius*) using response surface methodology. *J Food Process Pres* **38**:2090-2098 (2014).
8. Deng L, Mujumdar AS, Zhang Q, Yang X, Wang J, Zheng Z, Gao Z and Xiao H, Chemical and physical pretreatments of fruits and vegetables: Effects on drying characteristics and quality attributes - a comprehensive review. *Critical Rev Food Sci Nutri* **59**:1408-1432 (2019).
9. Osae R, Essilfie G, Alolga RN, Akaba S, Song X, Owusu-Ansah P and Zhou C, Application of non-thermal pretreatment techniques on agricultural products prior to drying: a review. *J Sci Food Agric* **100**:2585-2599 (2020).
10. Yang F, Zhang M, Mujumdar AS, Zhong Q and Wang Z, Enhancing drying efficiency and product quality using advanced pretreatments and analytical tools-An overview. *Drying Technol* **36**:1824-1838 (2018).
11. Chen F, Zhang M and Yang CH, Application of ultrasound technology in processing of ready-to-eat fresh food: A review. *Ultrason Sonochem* **63**:104953 (2020).
12. Musielak G, Mierzwa D and Kroehnke J, Food drying enhancement by ultrasound – A review. *Trends Food Sci Technol* **56**:126-141 (2016).
13. Gamboa-Santos J, Montilla A, Cárcel JA, Villamiel M and Garcia-Perez JV, Air-borne ultrasound application in the convective drying of strawberry. *J Food Eng* **128**:132-139 (2014).
14. Gamboa-Santos J, Montilla A, Soria AC, Carcel JA, Garcia-Perez JV and Villamiel M, Impact of power ultrasound on chemical and physicochemical quality indicators of strawberries dried by convection. *Food Chem* **161**:40-46 (2014).
15. Kowalski SJ, Pawłowski A, Szadzińska J, Łechtańska J and Stasiak M, High power airborne

- ultrasound assist in combined drying of raspberries. *Innov Food Sci Emerg* **34**:225-233 (2016).
16. Szadzińska J, Lechtanska J, Kowalski SJ and Stasiak M, The effect of high power airborne ultrasound and microwaves on convective drying effectiveness and quality of green pepper. *Ultrason Sonochem* **34**:531-539 (2017).
 17. Chen Y, Li M, Dharmasiri TSK, Song X, Liu F and Wang X, Novel ultrasonic-assisted vacuum drying technique for dehydrating garlic slices and predicting the quality properties by low field nuclear magnetic resonance. *Food Chem* **306**:125625 (2020).
 18. Liu Y, Zeng Y, Hu X and Sun X, Effect of ultrasonic power on water removal kinetics and moisture migration of kiwifruit slices during contact ultrasound intensified heat pump drying. *Food Bioprocess Technol* **13**:430-441 (2020).
 19. Baeghbali V, Niakousari M, Ngadi MO and Hadi Eskandari M, Combined ultrasound and infrared assisted conductive hydro-drying of apple slices. *Drying Technol* **37**:1793-1805 (2018).
 20. Guo Y, Wu B, Guo X, Ding F, Pan Z and Ma H, Effects of power ultrasound enhancement on infrared drying of carrot slices: Moisture migration and quality characterizations. *LWT-Food Sci Technol* **126**:109312 (2020).
 21. Feng Y, Zhou C, ElGasim A, Yagoub A, Sun Y, Owusu-Ansah P, Yu X, Wang X, Xu X, Zhang J and Ren Z, Improvement of the catalytic infrared drying process and quality characteristics of the dried garlic slices by ultrasound-assisted alcohol pretreatment. *LWT-Food Sci Technol* **116** (2019).
 22. Xi H, Liu Y, Guo L and Hu R, Effect of ultrasonic power on drying process and quality properties of far-infrared radiation drying on potato slices. *Food Sci Biotechnol* **29**:93-101 (2020).
 23. Zhang Z, Niu L, Li D, Liu C, Ma R, Song J and Zhao J, Low intensity ultrasound as a pretreatment to drying of daylilies: Impact on enzyme inactivation, color changes and nutrition quality parameters. *Ultrason Sonochem* **36**:50-58 (2017).
 24. Li L, Zhang M and Wang W, Ultrasound-assisted osmotic dehydration pretreatment before pulsed fluidized bed microwave freeze-drying (PFBMFD) of Chinese yam. *Food Biosci* **35**:100548 (2020).

25. Başlar M, Kılıçlı M, Toker OS, Sağdıç O and Arici M, Ultrasonic vacuum drying technique as a novel process for shortening the drying period for beef and chicken meats. *Innov Food Sci Emerg* **26**:182-190 (2014).
26. Santacatalina JV, Guerrero ME, Garcia-Perez JV, Mulet A and Cárcel JA, Ultrasonically assisted low-temperature drying of desalted codfish. *LWT - Food Sci Technol* **65**:444-450 (2016).
27. Başlar M, Kilicli M and Yalinkilic B, Dehydration kinetics of salmon and trout fillets using ultrasonic vacuum drying as a novel technique. *Ultrason Sonochem* **27**:495-502 (2015).
28. Huang D, Men K, Li D, Wen T, Gong Z, Sunden B and Wu Z, Application of ultrasound technology in the drying of food products. *Ultrason Sonochem* **63**:104950 (2020).
29. Xu F, Jin X, Zhang L and Chen XD, Investigation on water status and distribution in broccoli and the effects of drying on water status using NMR and MRI methods. *Food Res Int* **96**:191-197 (2017).
30. Cheng S, Zhang T, Yao L, Wang X, Song Y, Wang H, Wang H and Tan M, Use of low-field-NMR and MRI to characterize water mobility and distribution in pacific oyster (*Crassostrea gigas*) during drying process. *Drying Technol* **36**:630-636 (2018).
31. Ojha KS, Kerry JP and Tiwari BK, Investigating the influence of ultrasound pre-treatment on drying kinetics and moisture migration measurement in *Lactobacillus sakei* cultured and uncultured beef jerky. *LWT - Food Sci Technol* **81**:42-49 (2017).
32. Li L, Zhang M and Yang P, Suitability of LF-NMR to analysis water state and predict dielectric properties of Chinese yam during microwave vacuum drying. *LWT-Food Sci Technol* **105**:257-264 (2019).
33. Song Y, Zang X, Kamal T, Bi J, Cong S, Zhu B and Tan M, Real-time detection of water dynamics in abalone (*Haliotis discus hannai* Ino) during drying and rehydration processes assessed by LF-NMR and MRI. *Drying Technol* **36**:72-83 (2018).
34. Cheng S, Tang Y, Zhang T, Song Y, Wang X, Wang H, Wang H and Tan M, Approach for monitoring the dynamic states of water in shrimp during drying process with LF-NMR and MRI. *Drying Technol* **36**:841-848 (2017).

35. Ju H, Zhao S, Mujumdar AS, Fang X, Gao Z, Zheng Z and Xiao H, Energy efficient improvements in hot air drying by controlling relative humidity based on Weibull and Bi-Di models. *Food Bioprod Process* **111**:20-29 (2018).
36. Wang J, Yang X, Mujumdar AS, Wang D, Zhao J, Fang X, Zhang Q, Xie L, Gao Z and Xiao H, Effects of various blanching methods on weight loss, enzymes inactivation, phytochemical contents, antioxidant capacity, ultrastructure and drying kinetics of red bell pepper (*Capsicum annuum* L.). *LWT-Food Sci Technol* **77**:337-347 (2017).
37. Traffano-Schiffo MV, Castro-Giráldez M, Fito PJ and Balaguer N, Thermodynamic model of meat drying by infrared thermography. *J Food Eng* **128**:103-110 (2014).
38. Bantle M and Eikevik TM, A study of the energy efficiency of convective drying systems assisted by ultrasound in the production of clipfish. *J Clean Prod* **65**:217-223 (2014).
39. Corzo O, Bracho N, Pereira A and Vásquez A, Weibull distribution for modeling air drying of coroba slices. *LWT - Food Sci Technol* **41**:2023-2028 (2008).
40. Gerhards C, Schramm M and Schmid A, Use of the Weibull distribution function for describing cleaning kinetics of high pressure water jets in food industry. *J Food Eng* **253**:21-26 (2019).
41. Li M, Wang H, Zhao G, Qiao M, Li M, Sun L, Gao X and Zhang J, Determining the drying degree and quality of chicken jerky by LF-NMR. *J Food Eng* **139**:43-49 (2014).
42. Zhang J, Zhou D, Zhong X, Pei Z, Tian Y, Xiang D, Cao J, Shen X and Li C, Quality and protein degradation of golden pompano (*Trachinotus blochii*) fillets during four drying methods. *LWT-Food Sci Technol* **130** (2020).
43. Szadzińska J, Mierzwa D, Pawłowski A, Musielak G, Pashminehazar R and Kharaghani A, Ultrasound- and microwave-assisted intermittent drying of red beetroot. *Drying Technol* **38**:93-107 (2019).
44. Ozuna C, Puig A, Garcia-Perez JV and Cárcel JA, Ultrasonically enhanced desalting of cod (*Gadus morhua*). Mass transport kinetics and structural changes. *LWT - Food Sci Technol* **59**:130-137 (2014).

Figure Captions

Figure 1. Effect of ultrasound pretreatment on the drying kinetics of scallop adductors during heat pump drying. (a) drying curves, and (b) drying rate curves.

Figure 2. Typical LF-NMR transverse relaxation time (T_2) spectra of fresh scallop adductors.

Figure 3. Effect of ultrasound pretreatment on the water state and distribution of scallop adductors during heat pump drying. (a) ultrasound power 0 W (CK), (b) ultrasound power 90 W (US-90), and (c) ultrasound power 180 W (US-180).

Figure 4. Effect of US pretreatment on the cumulative percentage of free water, immobilized water, and bound water of scallop adductors. (a) US power 0 W (CK), (b) US power 90 W (US-90), and (c) US power 180 W (US-180).

Figure 5. Correlations analysis between transverse relaxation time of immobilized water (T_{22}) and the total moisture content of scallop adductors.

Figure 6. Principal components score plot of heat pump dried scallop adductors based on the obtained LF-NMR parameters.

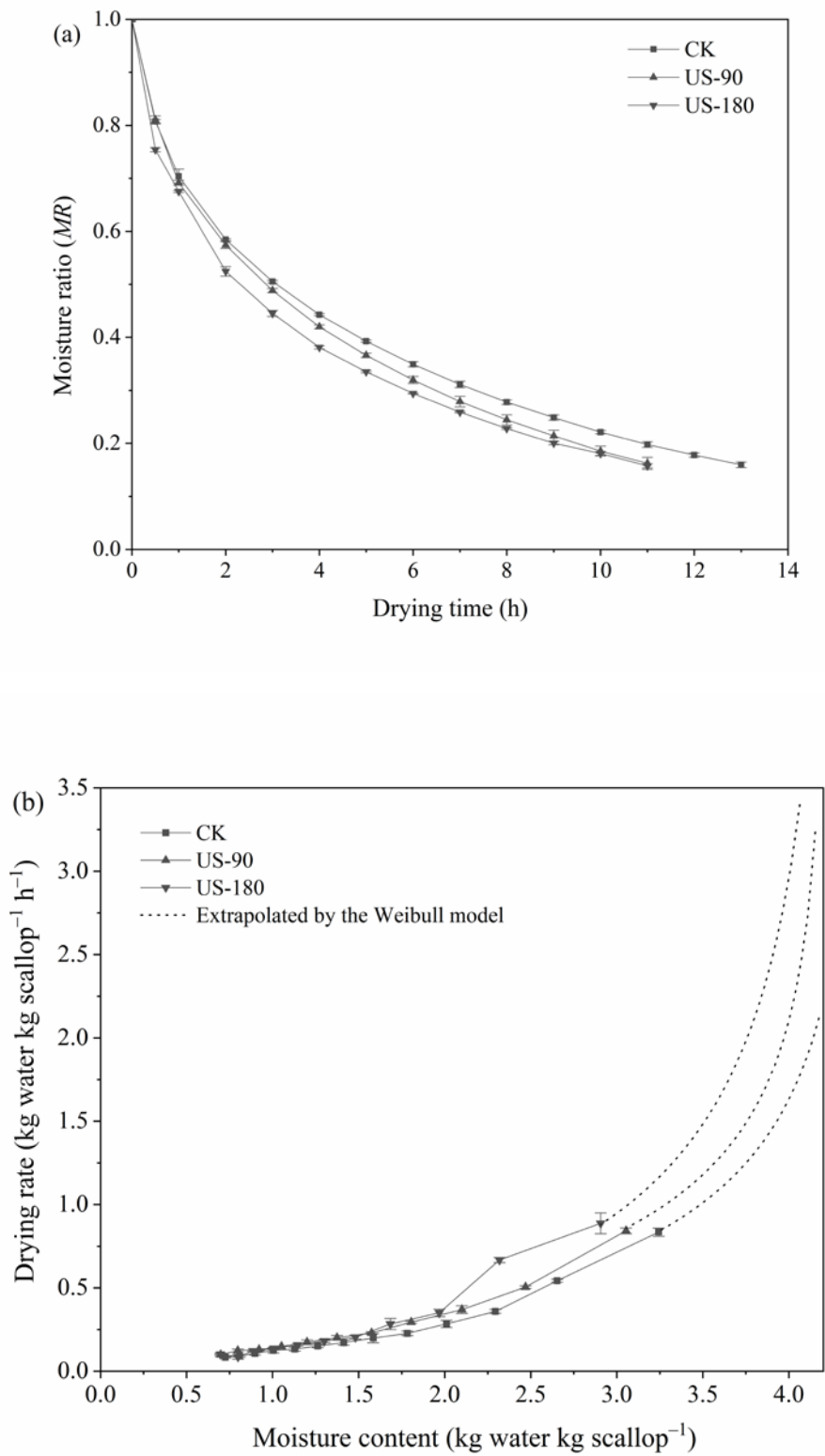


Figure 1. Effect of ultrasound pretreatment on the drying kinetics of scallop adductors

during heat pump drying. (a) drying curves, and (b) drying rate curves.

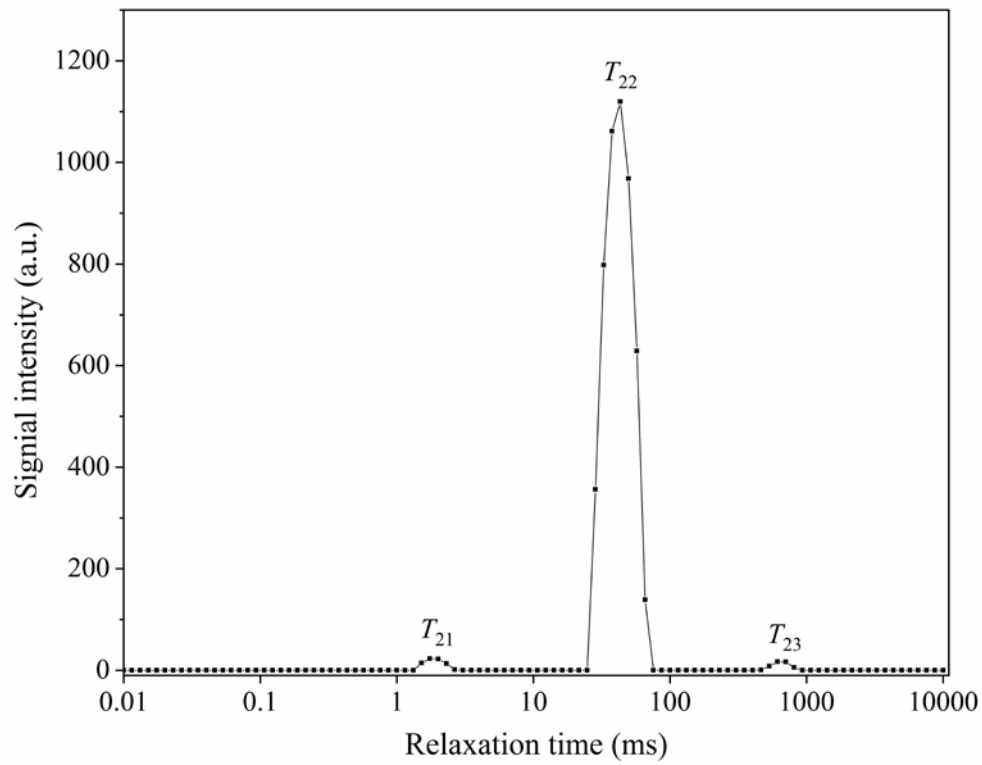
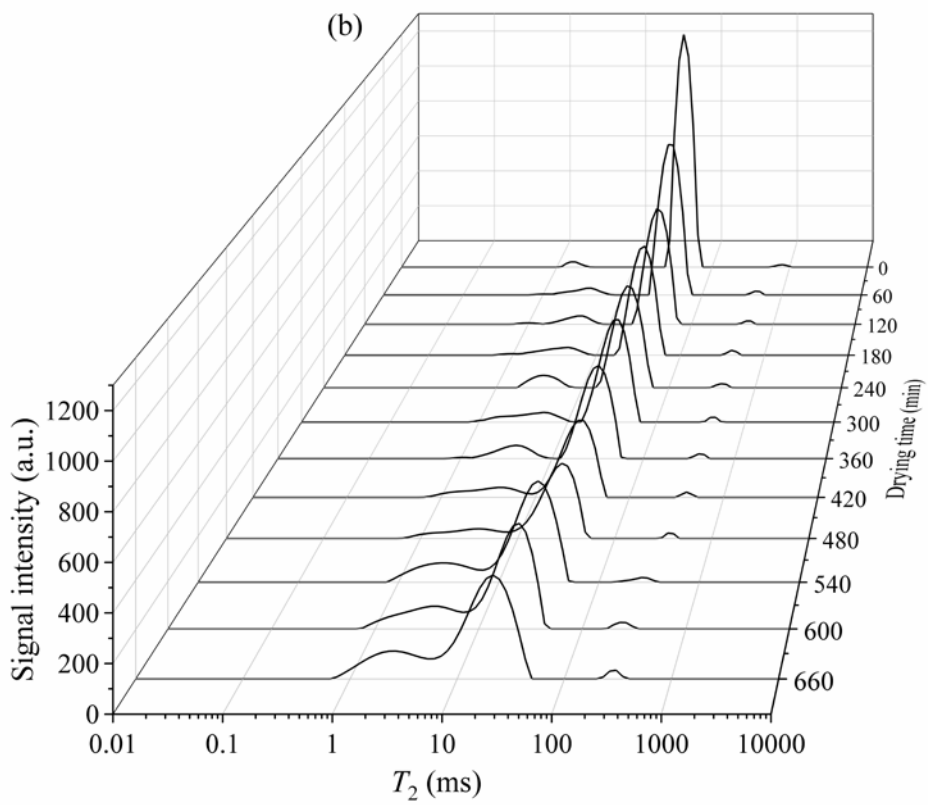
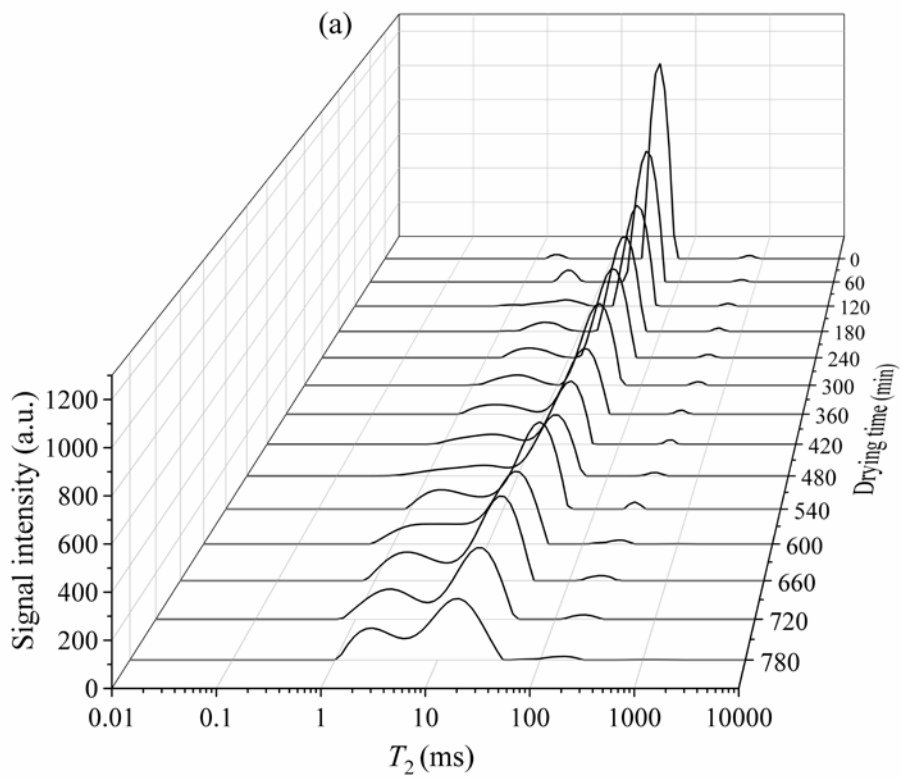


Figure 2. Typical LF-NMR transverse relaxation time (T_2) spectra of fresh scallop adductors.



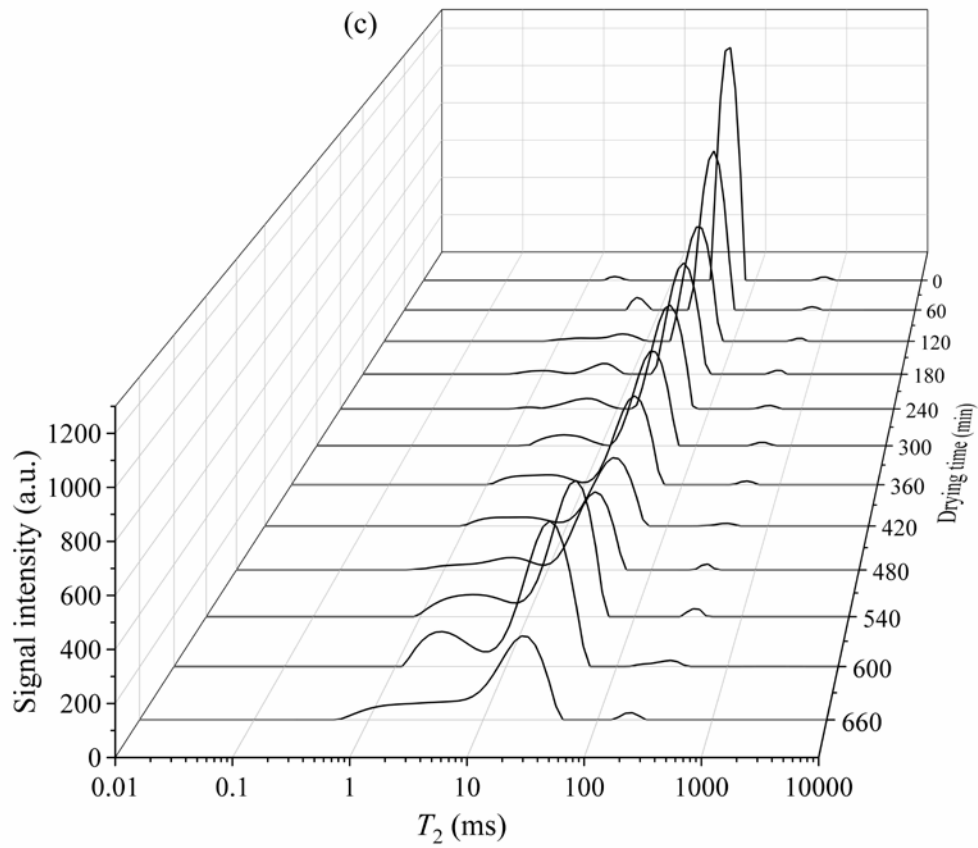
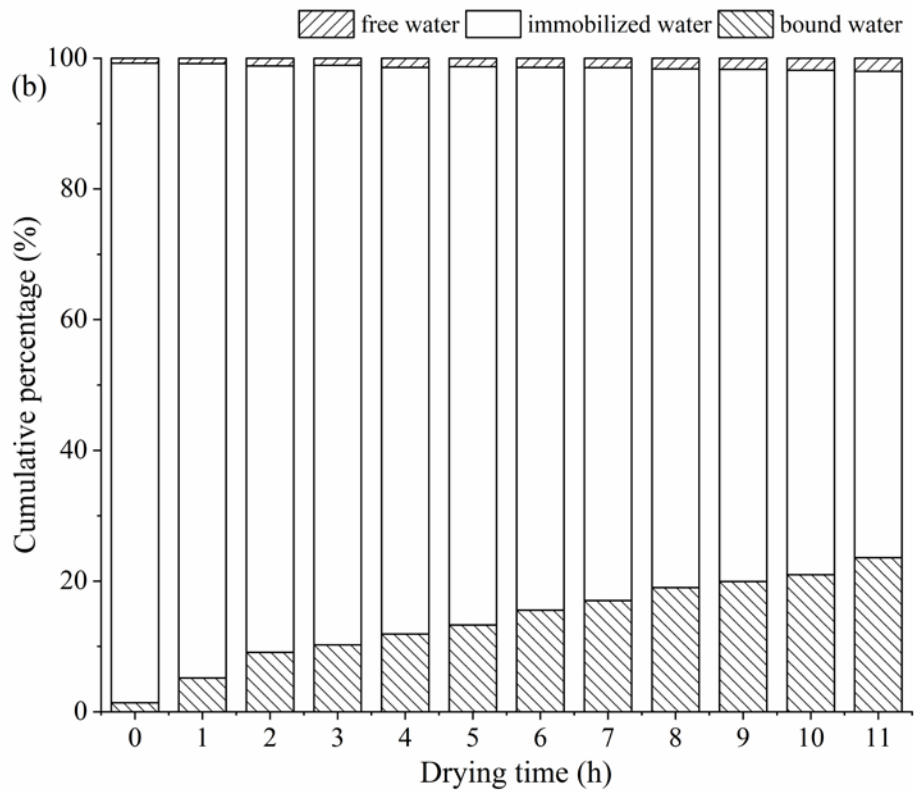
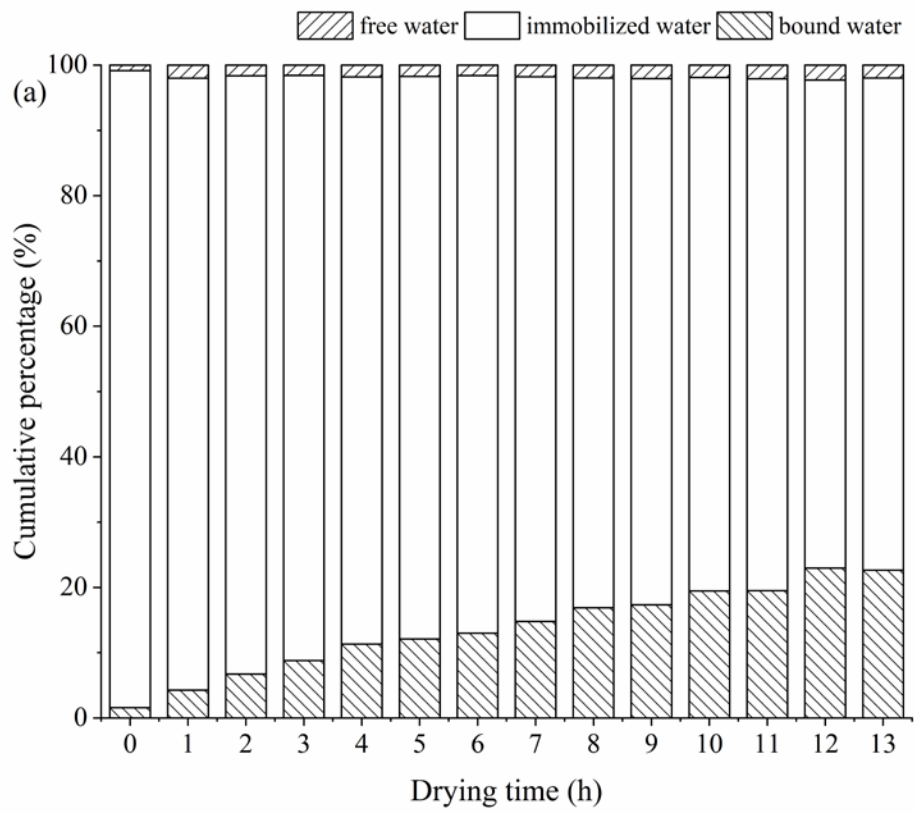


Figure 3. Effect of ultrasound pretreatment on the water state and distribution of scallop adductors during heat pump drying. (a) ultrasound power 0 W (CK), (b) ultrasound power 90 W (US-90), and (c) ultrasound power 180 W (US-180).



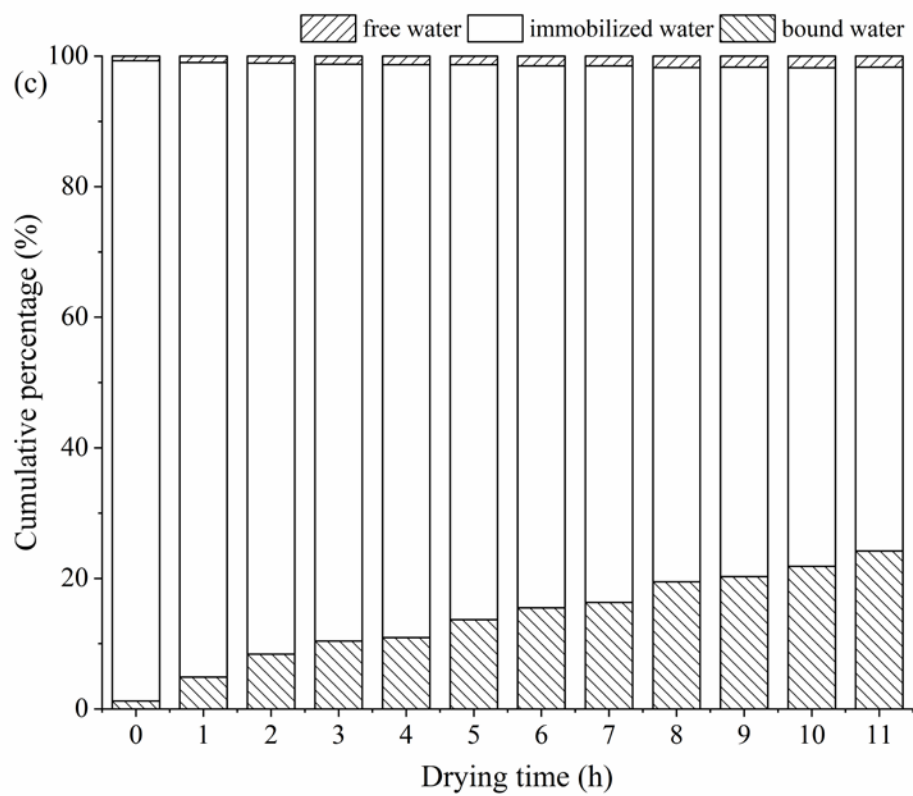


Figure 4. Effect of US pretreatment on the cumulative percentage of free water, immobilized water, and bound water of scallop adductors. (a) US power 0 W (CK), (b) US power 90 W (US-90), and (c) US power 180 W (US-180).

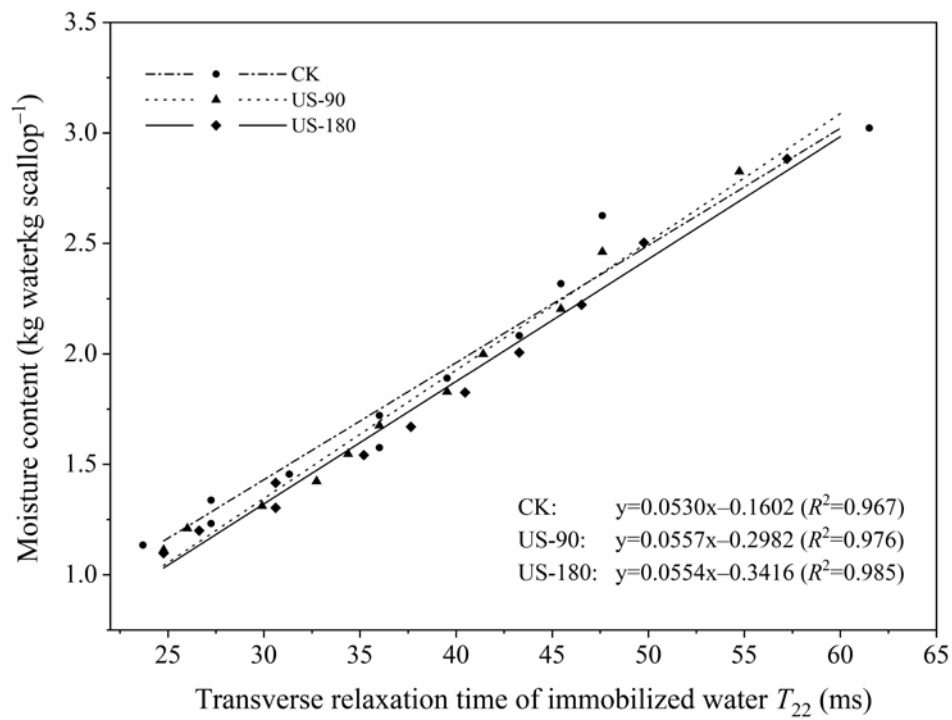


Figure 5. Correlations analysis between transverse relaxation time of immobilized water (T_{22}) and the total moisture content of scallop adductors.

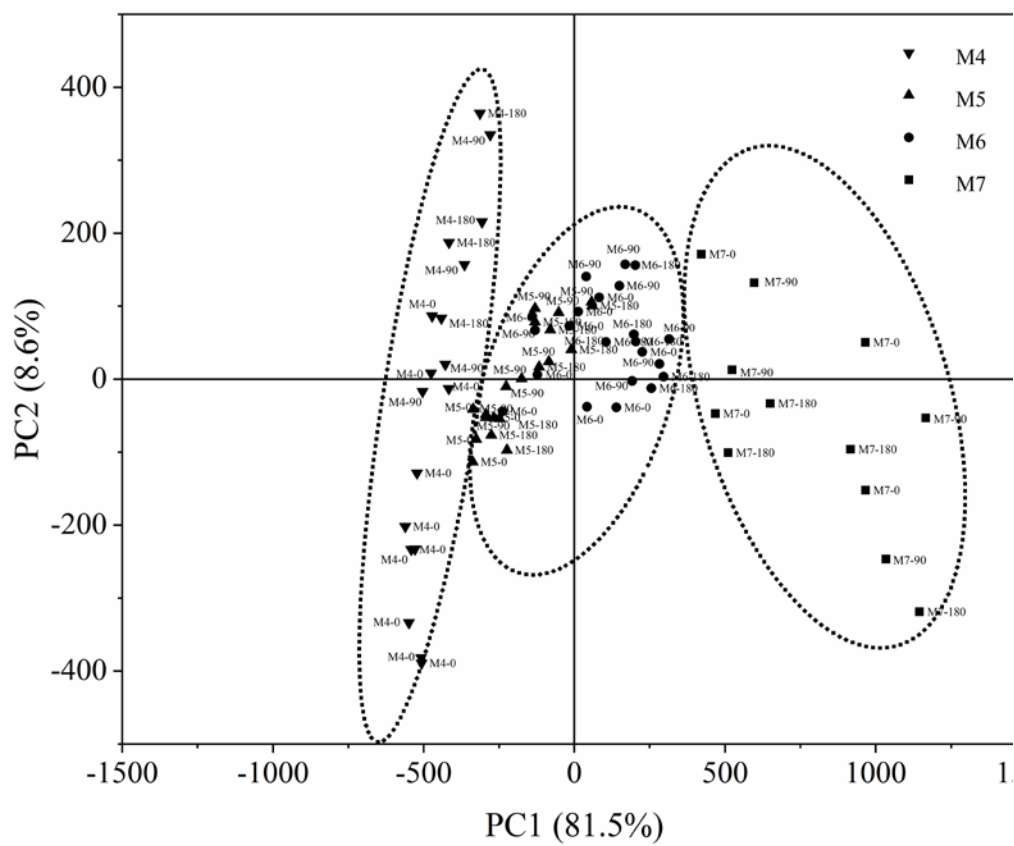


Figure 6. Principal components score plot of heat pump dried scallop adductors based on the obtained LF-NMR parameters.

Figure Captions

Figure 1. Effect of ultrasound pretreatment on the drying kinetics of scallop adductors during heat pump drying. (a) drying curves, and (b) drying rate curves.

Figure 2. Typical LF-NMR transverse relaxation time (T_2) spectra of fresh scallop adductors.

Figure 3. Effect of ultrasound pretreatment on the water state and distribution of scallop adductors during heat pump drying. (a) ultrasound power 0 W (CK), (b) ultrasound power 90 W (US-90), and (c) ultrasound power 180 W (US-180).

Figure 4. Effect of US pretreatment on the cumulative percentage of free water, immobilized water, and bound water of scallop adductors. (a) US power 0 W (CK), (b) US power 90 W (US-90), and (c) US power 180 W (US-180).

Figure 5. Correlations analysis between transverse relaxation time of immobilized water (T_{22}) and the total moisture content of scallop adductors.

Figure 6. Principal components score plot of heat pump dried scallop adductors based on the obtained LF-NMR parameters.

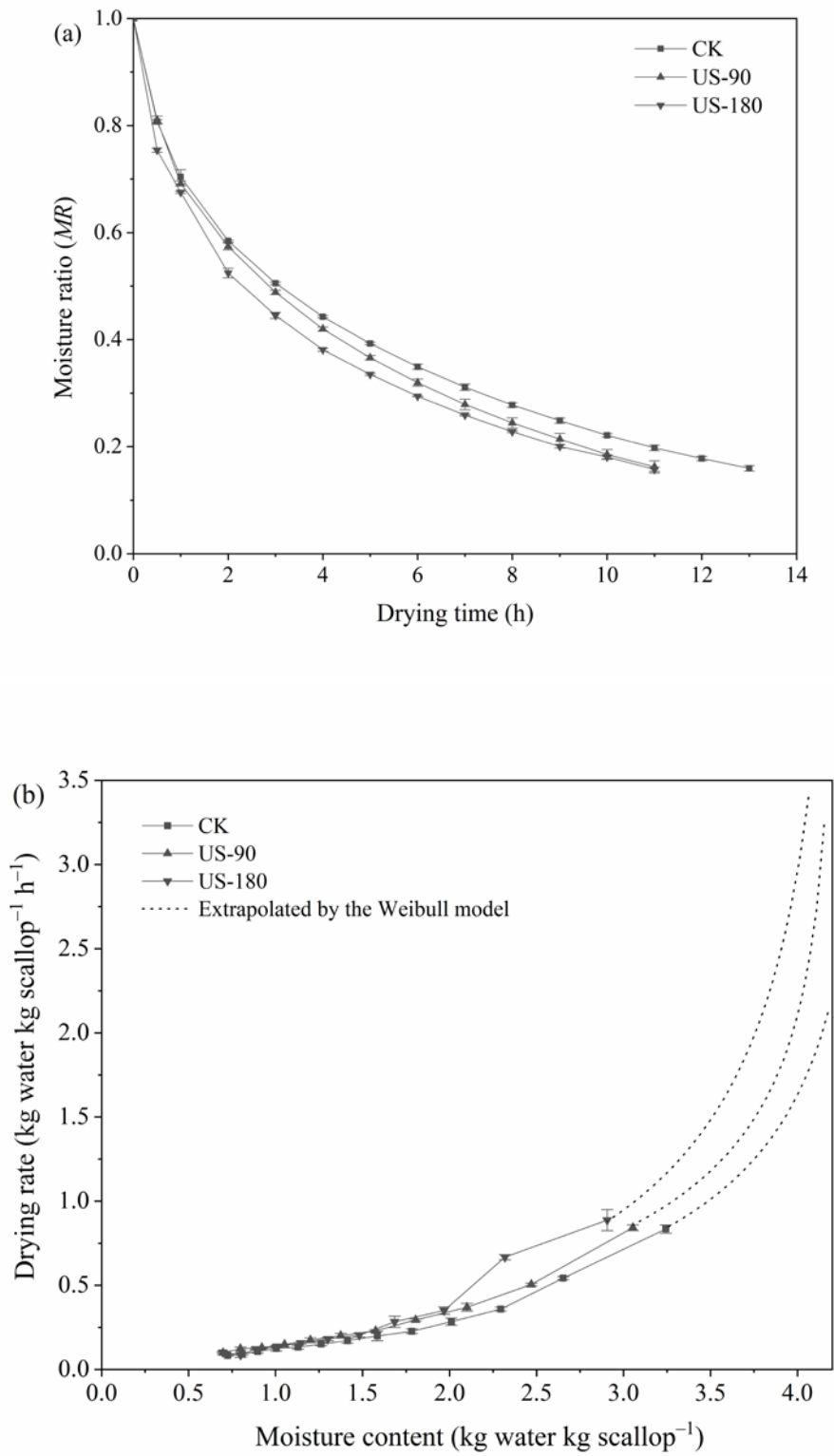


Figure 1. Effect of ultrasound pretreatment on the drying kinetics of scallop adductors during heat pump drying. (a) drying curves, and (b) drying rate curves.

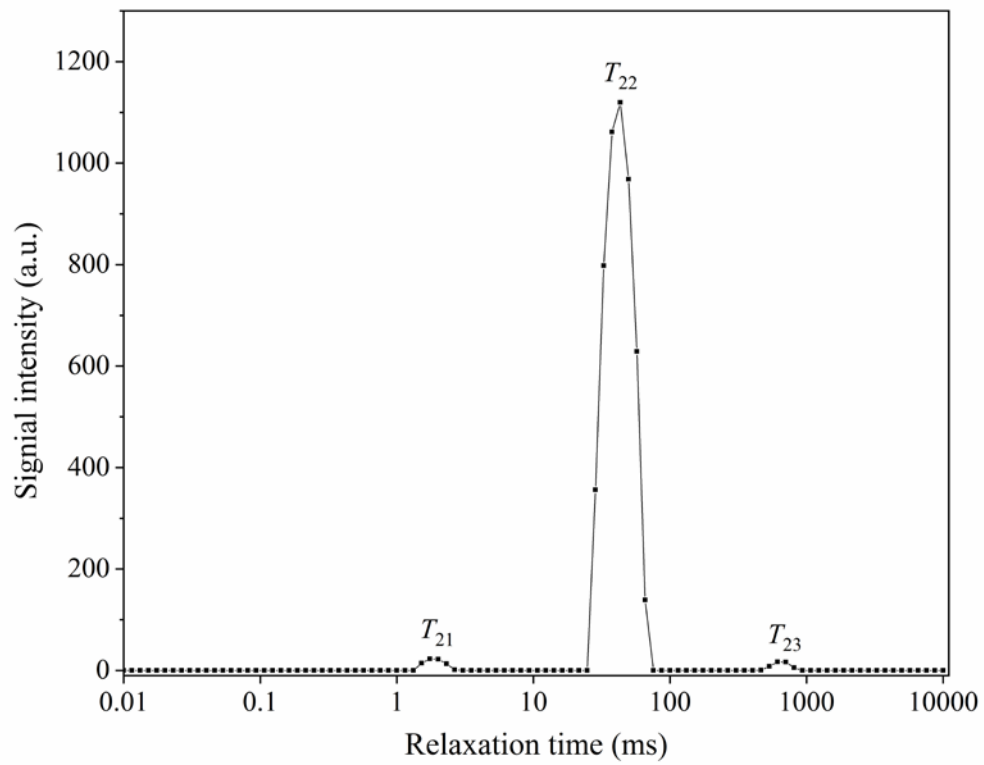
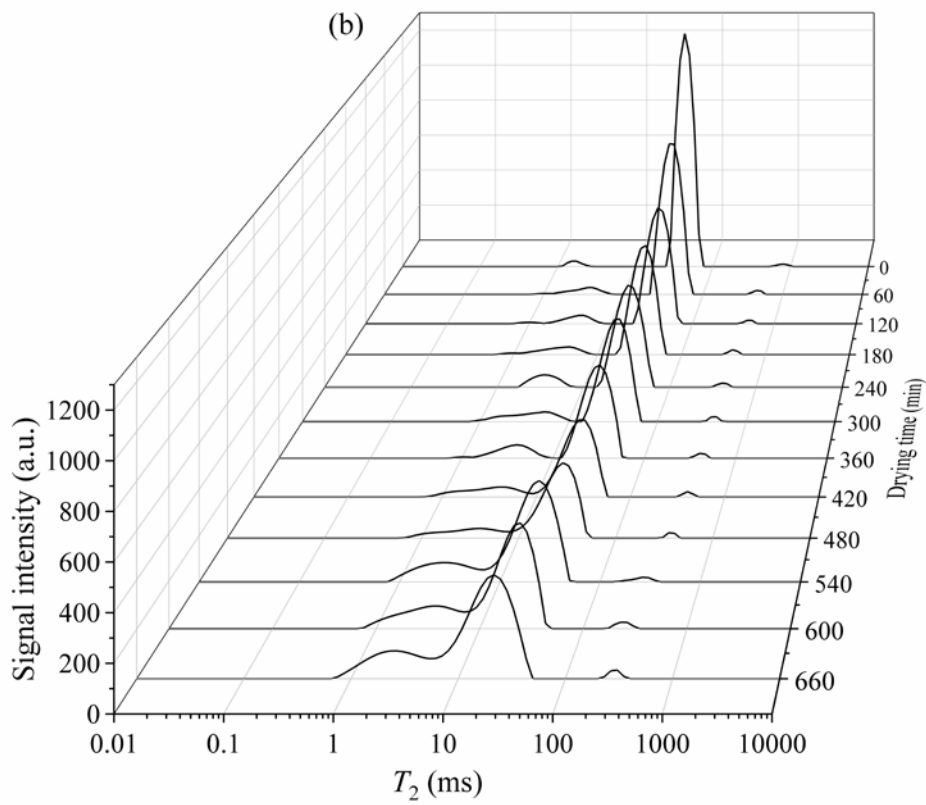
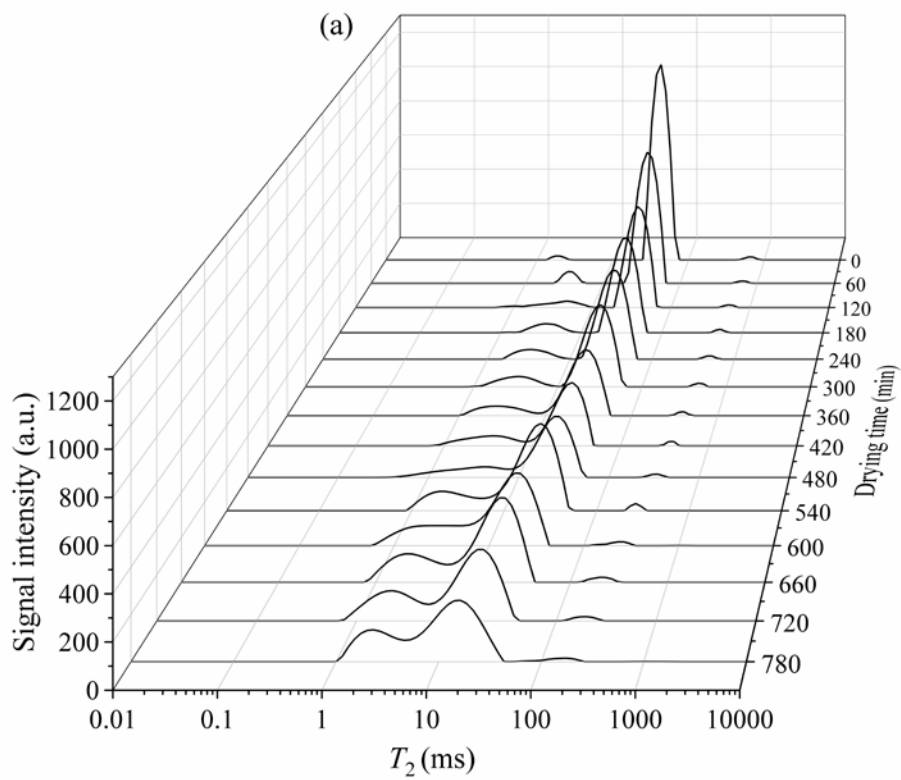


Figure 2. Typical LF-NMR transverse relaxation time (T_2) spectra of fresh scallop adductors.



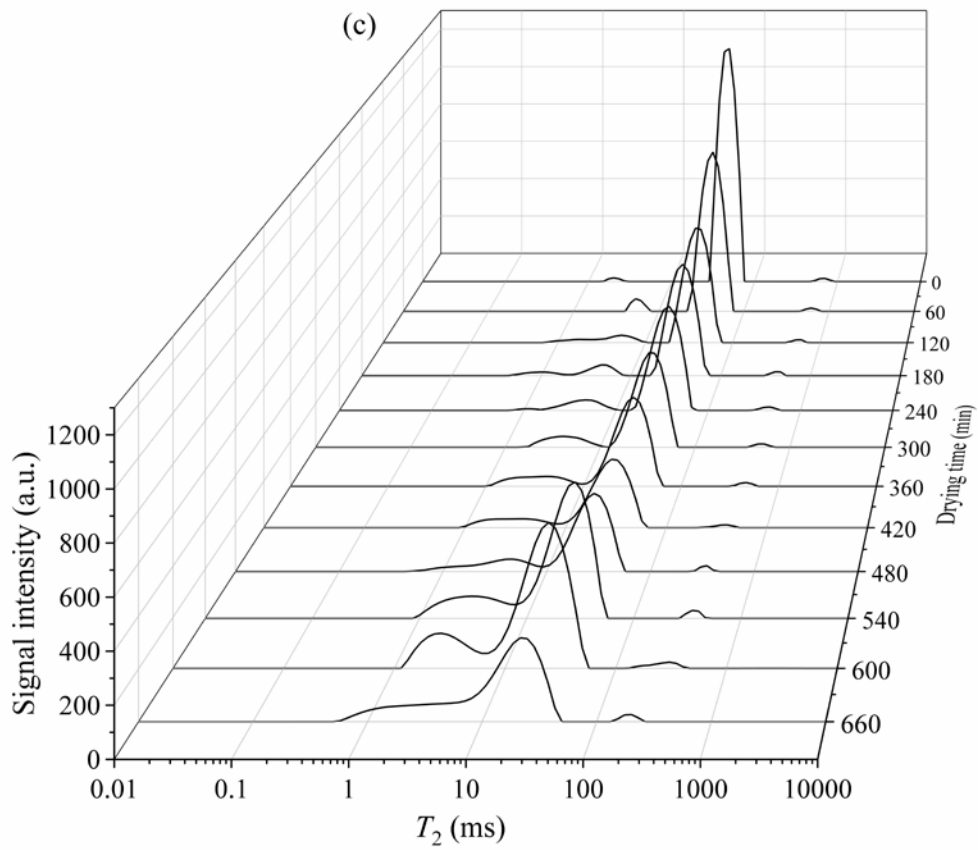
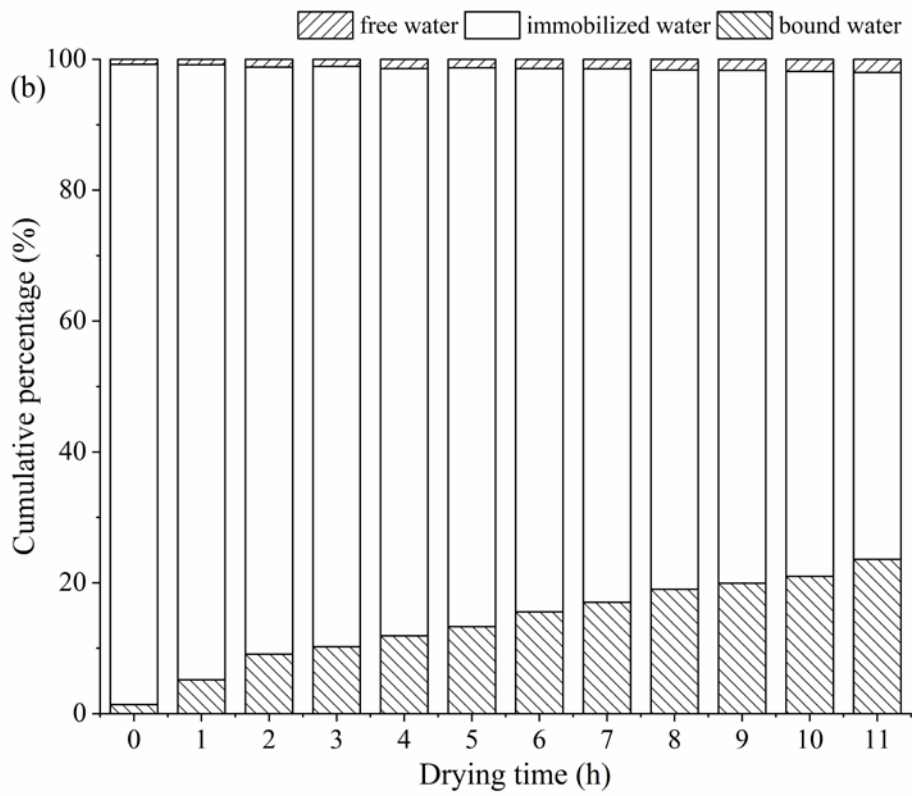
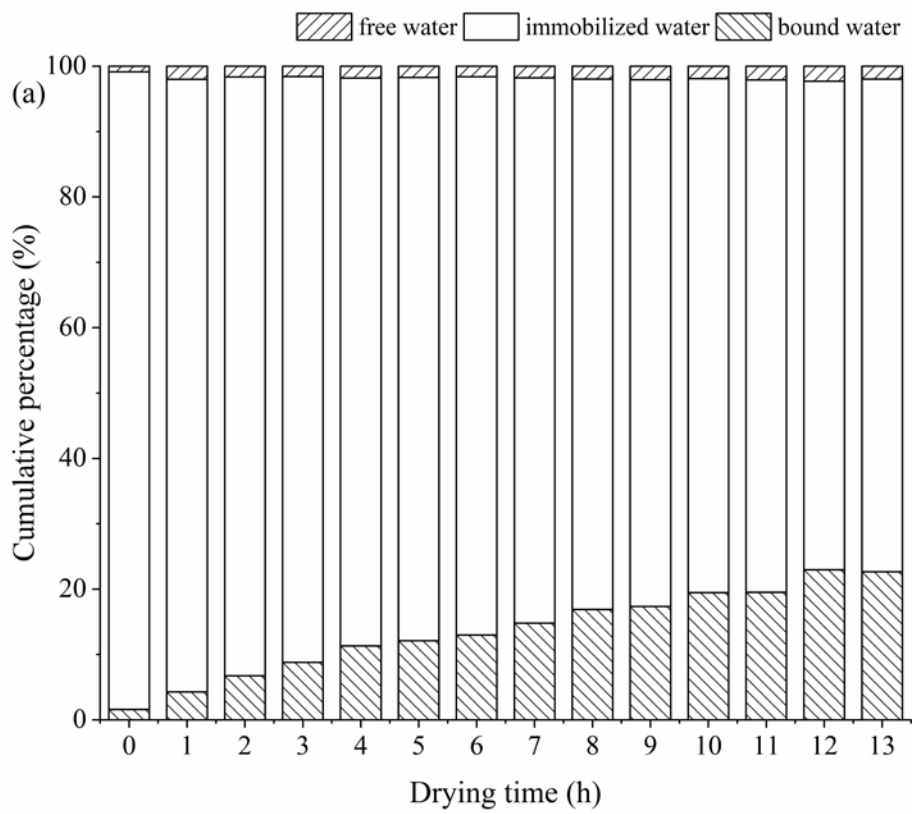


Figure 3. Effect of ultrasound pretreatment on the water state and distribution of scallop adductors during heat pump drying. (a) ultrasound power 0 W (CK), (b) ultrasound power 90 W (US-90), and (c) ultrasound power 180 W (US-180).



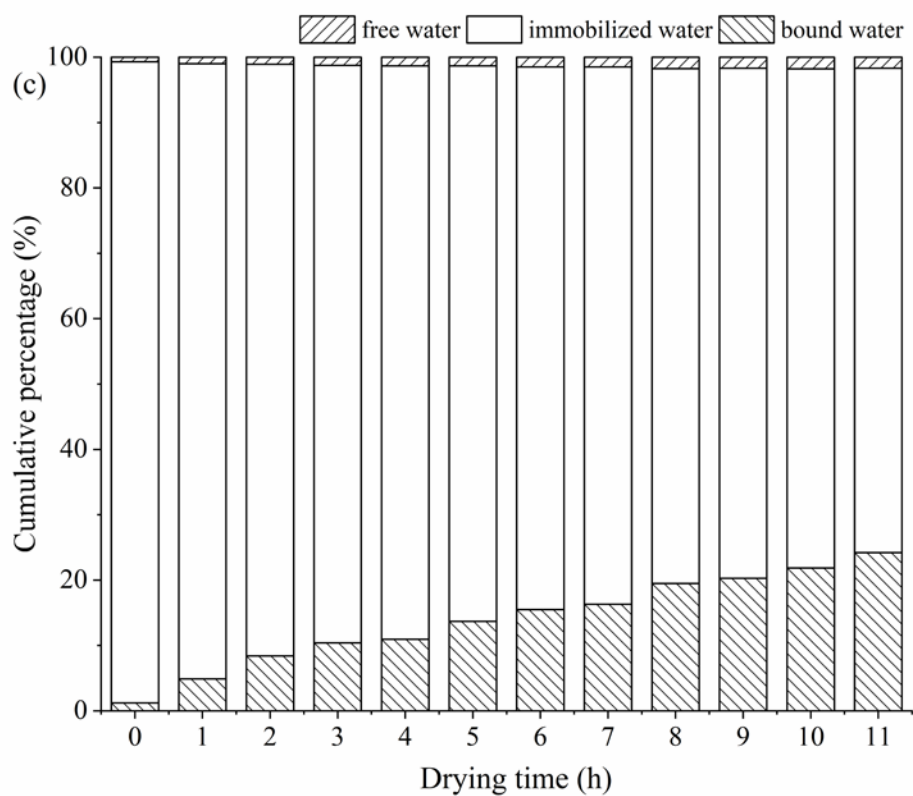


Figure 4. Effect of US pretreatment on the cumulative percentage of free water, immobilized water, and bound water of scallop adductors. (a) US power 0 W (CK), (b) US power 90 W (US-90), and (c) US power 180 W (US-180).

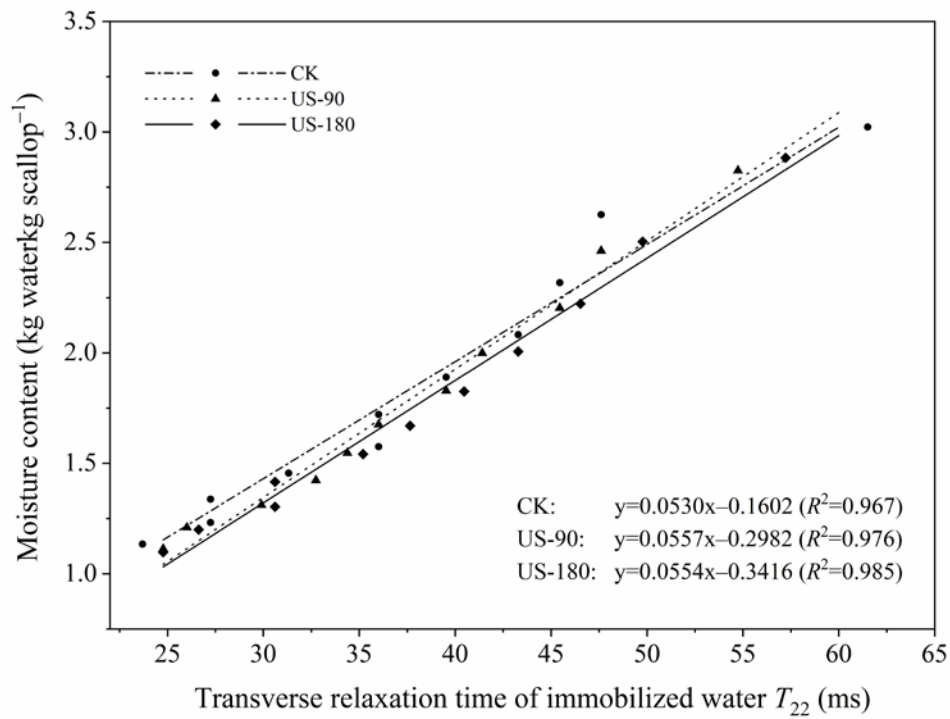


Figure 5. Correlations analysis between transverse relaxation time of immobilized water (T_{22}) and the total moisture content of scallop adductors.

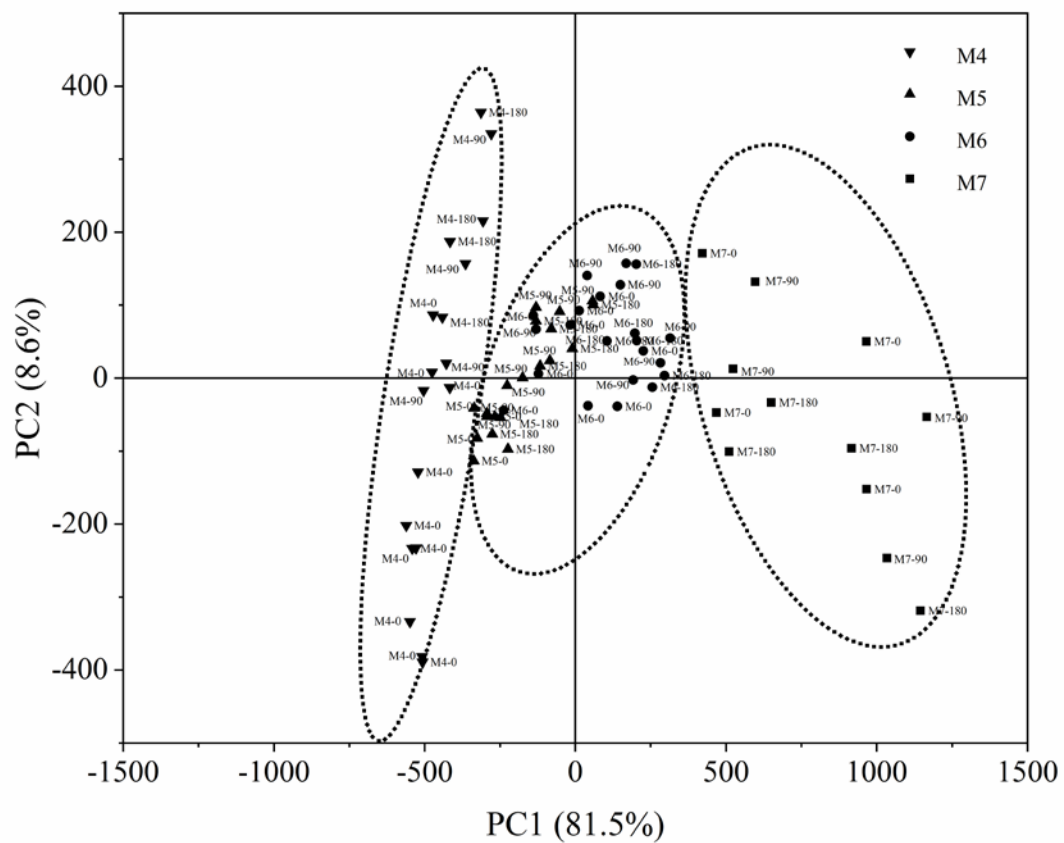


Figure 6. Principal components score plot of heat pump dried scallop adductors based on the obtained LF-NMR parameters.

Table Captions

Table 1. Effect of ultrasonic pretreatment on the regression parameters and statistical test of the Weibull model

Table 2. Effect of ultrasonic pretreatment on the quality attributes of heat pump dried scallop adductors

Table 1. Effect of ultrasonic pretreatment on the regression parameters and statistical test of the Weibull model

Treatment	α (min)	β	R^2	$RMSE$	$\chi^2 (\times 10^{-5})$	$D_{eff} (\times 10^{-10} \text{ m}^2 \text{ s}^{-1})$
CK	322.57 \pm 19.39 ^a	0.65 \pm 0.05 ^a	0.999	0.0107	7.143	2.933
US-90	287.25 \pm 7.80 ^b	0.69 \pm 0.03 ^a	0.999	0.0120	8.140	3.365
US-180	246.92 \pm 14.77 ^c	0.60 \pm 0.07 ^a	0.999	0.0109	7.896	3.692

Data are shown in mean \pm standard deviation (n=3).

Means within each column with different lowercase superscript letters are significantly different ($P < 0.05$).

Note: CK, scallop adductors without ultrasound treatment; US-90, scallop adductors treated with ultrasound power 90 W; US-180, scallop adductors treated with ultrasound power 180 W.

α , the scale parameter of the Weibull model; β , the shape parameter of the Weibull model; R^2 , the coefficient of determination;

$RMSE$, root-mean-square error; χ^2 , chi-square; D_{eff} , effective moisture diffusion coefficient.

Table 2. Effect of ultrasonic pretreatment on the quality attributes of heat pump dried scallop adductors

Treatment	ΔE	R_R	S_R (%)	Hardness (g)	Toughness (g)
CK	18.03 \pm 0.09 ^a	1.18 \pm 0.08 ^a	69.06 \pm 1.33 ^a	151.52 \pm 5.26 ^a	2758.70 \pm 92.94 ^b
US-90	15.20 \pm 0.89 ^b	1.16 \pm 0.04 ^a	68.77 \pm 0.31 ^a	140.05 \pm 9.32 ^{ab}	3411.32 \pm 314.80 ^a
US-180	13.00 \pm 0.67 ^c	1.19 \pm 0.07 ^a	68.92 \pm 1.82 ^a	128.52 \pm 1.20 ^b	3006.80 \pm 223.75 ^{ab}

Data are shown in mean \pm standard deviation (n=3).

Means within each column with different lowercase superscript letters are significantly different ($P < 0.05$).

Note: CK, scallop adductors without ultrasound treatment; US-90, scallop adductors treated with ultrasound power 90 W;

US-180, scallop adductors treated with ultrasound power 180 W.

ΔE , total color difference; R_R , rehydration ratio; S_R , shrinkage rate.